

Molecular Mechanisms of Non-ionotropic NMDA Receptor Signaling in Dendritic Spine Shrinkage

Ivar S. Stein, Deborah K. Park,  Juan C. Flores,  Jennifer N. Jahncke, and Karen Zito

Center for Neuroscience, University of California, Davis, Davis, California 95618

Structural plasticity of dendritic spines is a key component of the refinement of synaptic connections during learning. Recent studies highlight a novel role for the NMDA receptor (NMDAR), independent of ion flow, in driving spine shrinkage and LTD. Yet little is known about the molecular mechanisms that link conformational changes in the NMDAR to changes in spine size and synaptic strength. Here, using two-photon glutamate uncaging to induce plasticity at individual dendritic spines on hippocampal CA1 neurons from mice and rats of both sexes, we demonstrate that p38 MAPK is generally required downstream of non-ionotropic NMDAR signaling to drive both spine shrinkage and LTD. In a series of pharmacological and molecular genetic experiments, we identify key components of the non-ionotropic NMDAR signaling pathway driving dendritic spine shrinkage, including the interaction between NOS1AP (nitric oxide synthase 1 adaptor protein) and neuronal nitric oxide synthase (nNOS), nNOS enzymatic activity, activation of MK2 (MAPK-activated protein kinase 2) and cofilin, and signaling through CaMKII. Our results represent a large step forward in delineating the molecular mechanisms of non-ionotropic NMDAR signaling that can drive shrinkage and elimination of dendritic spines during synaptic plasticity.

Key words: dendritic spine; long-term depression; nitric oxide; NMDA receptor; structural plasticity; two-photon imaging

Significance Statement

Signaling through the NMDA receptor (NMDAR) is vitally important for the synaptic plasticity that underlies learning. Recent studies highlight a novel role for the NMDAR, independent of ion flow, in driving synaptic weakening and dendritic spine shrinkage during synaptic plasticity. Here, we delineate several key components of the molecular pathway that links conformational signaling through the NMDAR to dendritic spine shrinkage during synaptic plasticity.

Introduction

Activity-driven changes in neuronal connectivity are important for the experience-dependent remodeling of brain circuitry. In particular, the elimination of spine synapses is vital for the refinement of synaptic circuits throughout development and during learning. Indeed, an initial phase of spine formation and synaptogenesis during development is followed by a pruning phase leading to the removal of incorrect and redundant spine synapses (Wise et al., 1979; Holtmaat et al., 2005; Zuo et al., 2005). Furthermore, *in vivo* studies have shown that learning is associated with spine shrinkage and elimination, and that the

level of spine loss is directly correlated with improved behavioral performance (Yang et al., 2009; Lai et al., 2012). Shrinkage and loss of dendritic spines can be driven by glutamatergic signaling mechanisms leading to synaptic weakening through induction of long-term depression (LTD) via activation of the NMDA-type glutamate receptor (NMDAR; Okamoto et al., 2004; Zhou et al., 2004; Hayama et al., 2013; Oh et al., 2013; Wiegert and Oertner, 2013) or via activation of group I metabotropic glutamate receptors (mGluRs; Ramiro-Cortés and Israely, 2013; Wilkerson et al., 2018).

Recent studies have demonstrated that NMDAR-dependent LTD and spine shrinkage can occur independent of ion flux through the NMDAR. Several of these studies have shown that LTD and spine shrinkage induced by low-frequency glutamatergic stimulation are blocked by competitive glutamate binding site NMDAR antagonists, but persist in the presence of the glycine/D-serine binding site NMDAR antagonist 7-chlorokynureate (7-CK) or the pore blocker MK-801 (Nabavi et al., 2013; Stein et al., 2015; Carter and Jahr, 2016; Wong and Gray, 2018); but, it is important to note that other studies find contradictory results (Babiec et al., 2014; Volianskis et al., 2015; Sanderson et al., 2016). Furthermore, high-frequency glutamatergic stimulation that normally leads to

Received Jan. 8, 2020; revised Mar. 20, 2020; accepted Apr. 5, 2020.

Author contributions: I.S.S., D.K.P., J.C.F., and K.Z. designed research; I.S.S., D.K.P., J.C.F., and J.N.J. performed research; I.S.S., D.K.P., J.C.F., and J.N.J. analyzed data; I.S.S., D.K.P., and K.Z. wrote the paper.

The authors declare no competing financial interests.

This work was supported by National Institutes of Health Grant R01-NS-062736 (to K.Z.). J.C.F. was supported by an NIGMS-funded Pharmacology Training Program (T32 GM099608). We thank Dr. Yasunori Hayashi for the cofilin-related DNA constructs; Julie Culp and Lorenzo Tom for technical support and help with analysis; and Nicole Claiborne, Jinyoung Jang, and Samuel Peshow for critical reading of the manuscript.

Correspondence should be addressed to Karen Zito at kzito@ucdavis.edu.

<https://doi.org/10.1523/JNEUROSCI.0046-20.2020>

Copyright © 2020 the authors

LTP and spine growth instead has been found to drive LTD and spine shrinkage when ion flow through the NMDAR is blocked with 7-CK or MK-801 (Nabavi et al., 2013; Stein et al., 2015). Altogether, the findings from several studies support a model where glutamate binding to the NMDAR, in the absence of ion flux, is sufficient to drive LTD and dendritic spine shrinkage.

Little is known about the molecular signaling mechanisms that link glutamate-induced conformational changes of the NMDAR to the induction of LTD and spine shrinkage. Non-ionotropic NMDAR signaling in LTD requires basal levels of intracellular Ca^{2+} and causes the activation of p38 MAPK (Nabavi et al., 2013). p38 MAPK is required for dendritic spine shrinkage induced by conformational signaling through the NMDAR (Stein et al., 2015). Furthermore, glutamate or NMDA binding causes conformational changes in the NMDAR intracellular domains that lead to changes in its interaction with the downstream signaling molecules PP1 and CaMKII (Aow et al., 2015; Dore et al., 2015). While these experiments have offered insights into the nature of the conformational and protein interaction changes, the only molecules directly implicated in non-ionotropic NMDAR signaling during synaptic plasticity to date are p38 MAPK and basal levels of intracellular Ca^{2+} .

Here we used two-photon glutamate uncaging, time-lapse imaging, and whole-cell recordings to define the molecular mechanisms that link non-ionotropic NMDAR signaling to the shrinkage and elimination of dendritic spines. We show that p38 MAPK is generally required for spine shrinkage and synaptic weakening driven by non-ionotropic NMDAR signaling, which does not depend on signaling through AMPA receptors (AMPA receptors) or mGluRs. Furthermore, we show that non-ionotropic NMDAR signaling in spine shrinkage relies on neuronal nitric oxide synthase (nNOS) activation and on the interaction between nNOS and NOS1AP, linking p38 MAPK activation to the NMDAR signaling complex. Downstream of p38 MAPK, MAPK-activated protein kinase 2 (MK2) and cofilin are required. Finally, we show that spine shrinkage driven by non-ionotropic NMDAR signaling requires the activation of CaMKII. Our results delineate key components of the signaling pathway linking non-ionotropic NMDAR signaling to dendritic spine shrinkage.

Materials and Methods

Preparation and transfection of organotypic slice cultures. Organotypic hippocampal slices were prepared from postnatal day 6 (P6) to P8 Sprague Dawley rats or C57BL/6 mice of both sexes, as described previously (Stoppini et al., 1991). The cultures were transfected 1–3 d (EGFP alone) or 3–4 d [cofilin knockdown (KD) and rescue experiments] before imaging via biolistic gene transfer (180 psi), as described previously (Woods and Zito, 2008). We coated 6–8 mg of 1.6 μ m gold beads with 10–15 μ g of EGFP-N1 (Clontech) or 20 μ g of pSuper-cofilin1-shRNA + 20 μ g of pSuper-ADF-shRNA (Bosch et al., 2014) + 8 μ g pCAG-CyRFP1 (Addgene; Laviv et al., 2016) + 4 μ g of EGFP-N1 or 20 μ g of pSuper-cofilin1-shRNA + 20 μ g of pSuper-ADF-shRNA + 8 μ g of pCAG-CyRFP1 + 4 μ g of shRNA-insensitive cofilin1-EGFP (Bosch et al., 2014).

Preparation of acute slices. Acute hippocampal slices were prepared from P16 to P20 GFP-M mice (Feng et al., 2000) of both sexes. Coronal 400 μ m slices were cut (VT100S Vibratome, Leica) in cold choline chloride dissection solution containing the following (in mM): 110 choline chloride, 2.5 KCl, 25 NaHCO₃, 0.5 CaCl₂, 7 MgCl₂, 1.3 NaH₂PO₄, 11.6 sodium ascorbate, 3.1 sodium pyruvate, and 25 glucose, saturated with 95% O₂/5% CO₂. Slices were recovered for 45 min in 30°C oxygenated artificial CSF (ACSF) containing the following (in mM): 127 NaCl, 25

NaHCO₃, 1.25 NaH₂PO₄, 2.5 KCl, 25 glucose, 2 CaCl₂, and 1 MgCl₂, and then incubated at room temperature for an additional 45 min before imaging.

Time-lapse two-photon imaging. EGFP-transfected CA1 pyramidal neurons from acute (P16–P20) or cultured [14–18 d *in vitro* (DIV)] slices at depths of 10–50 μ m were imaged using a custom two-photon microscope (Woods et al., 2011) controlled with ScanImage (Pologruto et al., 2003). Image stacks (512 × 512 pixels; 0.02 μ m/pixel) with 1 μ m z-steps were collected. For each neuron, one segment of secondary or tertiary basal dendrite was imaged at 5 min intervals at 29°C in recirculating ACSF (in mM): 127 NaCl, 25 NaHCO₃, 1.2 NaH₂PO₄, 2.5 KCl, 25 D-glucose, aerated with 95% O₂/5% CO₂, ~310 mOsm, pH 7.2, with 0.001 TTX, 0 Mg²⁺, and 2 Ca²⁺. Cells were preincubated for at least 30 min with 100 μ M 7-CK (100 mM stock in H₂O), 10 μ M L-689560 (L-689; 15 mM stock in DMSO), 2 μ M SB203580 (4 mM stock in DMSO), 10 μ M NBQX (10 mM stock in H₂O), 45 μ M CPCCOEt (90 mM stock in DMSO), 15 μ M MPEP (5 mM stock in H₂O), 10 μ M CPP (10 mM stock in H₂O), 100 μ M NG-nitro-L-arginine (L-NNA; 200 mM stock in 0.25N HCl), or 10 μ M KN-62 (20 mM stock in DMSO), all from Tocris Bioscience; 10 μ M MK2 inhibitor III (20 mM stock in DMSO) from Cayman Chemical; or 5 μ M TAT-CN21 (5 mM stock in H₂O) purchased from Ulli Bayer, as indicated. Cells were preincubated for at least 60 min with 1 μ M peptides (2 mM stock in H₂O). Peptides L-TAT-GESV (NH₂-GRKKRRQRRRYAGQWGESV-COOH) and L-TAT-GASA (NH₂-GRKKRRQRRRYAGQWGASA-COOH) were obtained from GenicBio.

High-frequency uncaging stimulus. High-frequency uncaging (HFU) consisted of 60 pulses (720 nm; ~8–10 mW at the sample) of 2 ms duration at 2 Hz delivered in ACSF containing the following (in mM): 2 Ca²⁺, 0 Mg²⁺, 2.5 MNI-glutamate, and 0.001 TTX. The laser beam was parked at a point ~0.5–1 μ m from the spine head in the direction away from the dendrite. We selected healthy cells based on a test HFU stimulus, as follows: before the application of pharmacological reagents, a spine was probed for transient growth in response to HFU, and only those cells with responsive spines were used for experiments, which assessed uncaging-induced structural changes of spines on a different dendrite than the original test spine.

Image analysis. Estimated spine volume was measured from background-subtracted green fluorescence using the integrated pixel intensity of a boxed region surrounding the spine head, as described previously (Woods et al., 2011). All shown images are maximum projections of three-dimensional image stacks after applying a median filter (3 × 3) to the raw image data.

Electrophysiology. Whole-cell recordings ($V_{\text{hold}} = -65$ mV; series resistance, 20–40 M Ω) were obtained from visually identified CA1 pyramidal neurons in slice culture (14–18 DIV; depths of 10–50 μ m) at 25°C in ACSF containing the following (in mM): 2 CaCl₂, 1 MgCl₂, 0.001 TTX, 2.5 MNI-glutamate. 10 μ M L-689 or 100 μ M 7-CK was included as indicated. Recording pipettes (~7 M Ω) were filled with a cesium-based internal solution (in mM): 135 Cs-methanesulfonate, 10 HEPES, 10 Na₂ phosphocreatine, 4 MgCl₂, 4 Na₂-ATP, 0.4 Na-GTP, 3 Na L-ascorbate, 0.2 Alexa Fluor 488, and ~300 mOsm, ~pH 7.25). For each cell, baseline uncaging-induced EPSCs (uEPSCs) were recorded (five to six test pulses at 0.1 Hz, 720 nm, 1 ms duration, 8–10 mW at the sample) from two spines (2–12 μ m apart) on secondary or tertiary basal branches (50–120 μ m from the soma). The HFU stimulus was then applied to one spine, during which the cell was depolarized to 0 mV. Following the HFU stimulus, uEPSCs were recorded from both the target and neighboring spine at 5 min intervals for 25 min. uEPSC amplitudes from individual spines were quantified as the average from a 2 ms window centered on the maximum current amplitude within 50 ms following uncaging pulse.

Statistics. All data are represented as the mean \pm SEM. All statistics were calculated across cells. Statistical significance was set at $p < 0.05$ (two-tailed *t* test). All *p* and *n* values are presented in the Results section and figure legends. Sample sizes are based on previously published studies from our laboratory and standards in the field. Cells for each condition were obtained from at least three independent hippocampal acute slices or slice culture preparations of both sexes. Data analysis was performed blind to the experimental condition.

Results

p38 MAPK activity is required for spine shrinkage induced by non-ionicotropic NMDAR signaling

To determine the signaling molecules downstream of non-ionicotropic NMDAR function in spine shrinkage, we began by confirming a general role for p38 MAPK, the only protein identified to date as a required component of the non-ionicotropic NMDAR signaling cascade using a low-frequency stimulus paradigm. We recently reported that p38 MAPK, which has been shown to play a role in conventional NMDAR-dependent LTD induced by low-frequency stimulation (Zhu et al., 2002), is required downstream of non-ionicotropic NMDAR signaling to drive dendritic spine shrinkage induced by a low-frequency uncaging stimulus (Stein et al., 2015) that also induces single spine LTD (Oh et al., 2013).

To assess the generalizability of the requirement for p38 MAPK as a signaling molecule downstream of non-ionicotropic NMDAR function in spine shrinkage, we tested whether p38 MAPK was also required for spine shrinkage induced by high-frequency uncaging (HFU; 60 pulses of 2 ms duration at 2 Hz) of glutamate in the presence of the NMDAR glycine/D-serine site antagonist 7-CK. HFU normally leads to spine growth, but the presence of 7-CK, which blocks ion flow through the NMDAR but leaves glutamate binding intact, converts a normally spine growth-inducing HFU stimulus (Fig. 1A,B; vehicle (veh): $216.4 \pm 37.7\%$, $p = 0.027$, $t_{(5)} = 3.08$, paired two-tailed t test) into spine shrinkage. Indeed, we found that spine shrinkage induced by HFU in the presence of 7-CK (Fig. 1A,B,D; $72.0 \pm 5.1\%$, $p = 0.0003$, $t_{(10)} = 5.52$) was blocked by the p38 MAPK inhibitor SB203580 (SB; Fig. 1A,B,D; $114.3 \pm 4.7\%$, $p = 0.019$, $t_{(7)} = 3.04$). The size of unstimulated neighboring spines was not affected (Fig. 1A,B,D; veh, $101.8 \pm 6.1\%$; 7-CK, $104.7 \pm 2.2\%$; 7-CK + SB, $101.3 \pm 4.5\%$), excluding any acute independent effects of SB203580 on spine morphology. Thus, p38 MAPK is required for spine shrinkage driven by non-ionicotropic NMDAR signaling in response to both low-frequency and high-frequency glutamatergic stimuli.

Since HFU stimulation in the presence of 7-CK still allows partial AMPAR activation, we used $10 \mu\text{M}$ NBQX, a competitive AMPAR antagonist, to test whether spine shrinkage occurred independent of AMPAR activation. We found that spine shrinkage induced by HFU in the presence of $100 \mu\text{M}$ 7-CK and $10 \mu\text{M}$ NBQX (Fig. 1C,D; $61.9 \pm 11.3\%$, $p = 0.019$, $t_{(6)} = 3.17$) was not different from that observed with 7-CK alone. Furthermore, spine shrinkage was still observed when HFU was induced in the presence of $100 \mu\text{M}$ 7-CK, $10 \mu\text{M}$ NBQX, $15 \mu\text{M}$ MPEP, and $45 \mu\text{M}$ CPCCOEt (Fig. 1C,D; $79.6 \pm 5.7\%$, $p = 0.007$, $t_{(8)} = 3.61$), confirming our previous results that non-ionicotropic NMDAR-dependent spine shrinkage is also independent of group I mGluRs (Stein et al., 2015). In addition, spine shrinkage induced by HFU in the presence of $100 \mu\text{M}$ 7-CK is independent of the presence of 1 mM Mg^{2+} (Fig. 1C,D; $73.1 \pm 5.8\%$, $p = 0.006$, $t_{(5)} = 4.62$), but is completely blocked in the presence of $10 \mu\text{M}$ CPP (Fig. 1C,D; $114.2 \pm 9.3\%$, $p = 0.17$, $t_{(7)} = 1.52$), a competitive antagonist of the NMDAR glutamate binding site, confirming our model that glutamate binding to, but not ion flow through, the NMDAR is required for dendritic spine shrinkage.

p38 MAPK activity is required for LTD driven by non-ionicotropic NMDAR signaling at individual dendritic spines

Our results confirm that p38 MAPK is required for the shrinkage and elimination of individual dendritic spines driven by non-

ionicotropic NMDAR signaling (Stein et al., 2015), and others have shown that p38 MAPK is activated by non-ionicotropic NMDAR signaling in LTD (Nabavi et al., 2013). However, whether spine shrinkage induced by non-ionicotropic NMDAR signaling at individual dendritic spines is associated with long-term depression of synaptic strength, and whether it requires activation of p38 MAPK, remains unknown.

To test whether non-ionicotropic NMDAR-dependent signaling at individual dendritic spines also leads to LTD, we first needed to replace the glycine/D-serine site antagonist that we were using in our experiments because 7-CK strongly inhibits AMPAR currents (Leeson et al., 1992; Wong and Gray, 2018), making LTD experiments challenging. Compared with 7-CK, L-689 is a more potent and selective glycine/D-serine site antagonist (Leeson et al., 1992), which completely blocks NMDAR-dependent ion flow at $10 \mu\text{M}$ (compared with $100 \mu\text{M}$ for 7-CK) and shows reduced inhibition of glutamate uncaging-evoked currents (uEPSCs) from AMPARs (Fig. 2A; 7-CK: $22.7 \pm 2.8\%$ of baseline, $p < 0.0001$, $t_{(21)} = 27.22$, paired two-tailed t test; L-689: $64.4 \pm 5.6\%$ of baseline, $p = 0.0014$, $t_{(5)} = 6.41$). Before initiating electrophysiological experiments, we first confirmed that L-689, like 7-CK, converted HFU-induced spine growth to spine shrinkage, characteristic of non-ionicotropic NMDAR signaling. Indeed, HFU-induced spine shrinkage is observed in the presence of $10 \mu\text{M}$ L-689 (Fig. 2B,C; $57.3 \pm 11.7\%$, $p = 0.008$, $t_{(7)} = 3.65$, paired two-tailed t test) similar to that found with $100 \mu\text{M}$ 7-CK (Fig. 2B,C; $58.6 \pm 12.0\%$, $p = 0.018$, $t_{(5)} = 3.47$).

To test whether spine shrinkage induced by non-ionicotropic NMDAR signaling at individual dendritic spines is associated with LTD, we recorded uEPSCs from one target spine and one neighboring spine at 5 min intervals before and after HFU stimulation in the presence of L-689. We found that HFU stimulation in the presence of L-689 led to a long-term decrease in the amplitude of uEPSCs (Fig. 3A,B; $76.4 \pm 6.5\%$, $p = 0.009$, $t_{(7)} = 3.61$, paired two-tailed t test). This decrease in uEPSC amplitude was completely blocked by the application of the p38 MAPK inhibitor SB203580 (Fig. 3C,D; $105.7 \pm 6.0\%$, $p = 0.38$, $t_{(6)} = 0.94$). Non-ionicotropic NMDAR-dependent LTD was specific to the stimulated target spine, as uEPSC amplitude of the unstimulated neighboring spines did not change (Fig. 3A–D; L-689; $105.7 \pm 8.7\%$; L-689 + SB, $104.3 \pm 7.8\%$). Together, our results indicate that p38 MAPK activity is required for both spine shrinkage and LTD induced by non-ionicotropic NMDAR signaling.

NOS1AP interaction with nNOS, and nNOS enzymatic activity act downstream of conformational NMDAR signaling to drive dendritic spine shrinkage

To shed light on how p38 MAPK activation is driven by non-ionicotropic NMDAR signaling, we searched the literature for signaling proteins that could link the NMDAR to p38 MAPK activation. Intriguingly, nitric oxide synthase 1 adaptor protein (NOS1AP) was recently implicated in p38 MAPK activation during NMDA-induced excitotoxicity (Li et al., 2013). Notably, disruption of the interaction between NOS1AP and nNOS with a cell-permeant peptide, L-TAT-GESV, which does not interfere with nNOS anchoring to PSD-95, inhibited NMDAR-dependent p38 MAPK activation (Li et al., 2013, 2015).

We tested whether L-TAT-GESV interferes with dendritic spine shrinkage driven by non-ionicotropic NMDAR signaling. We found that the application of L-TAT-GESV completely blocked spine shrinkage induced by HFU in the presence of 7-CK (Fig. 4A–C; $102.1 \pm 9.1\%$, $p = 0.82$, $t_{(14)} = 0.23$, paired two-tailed t

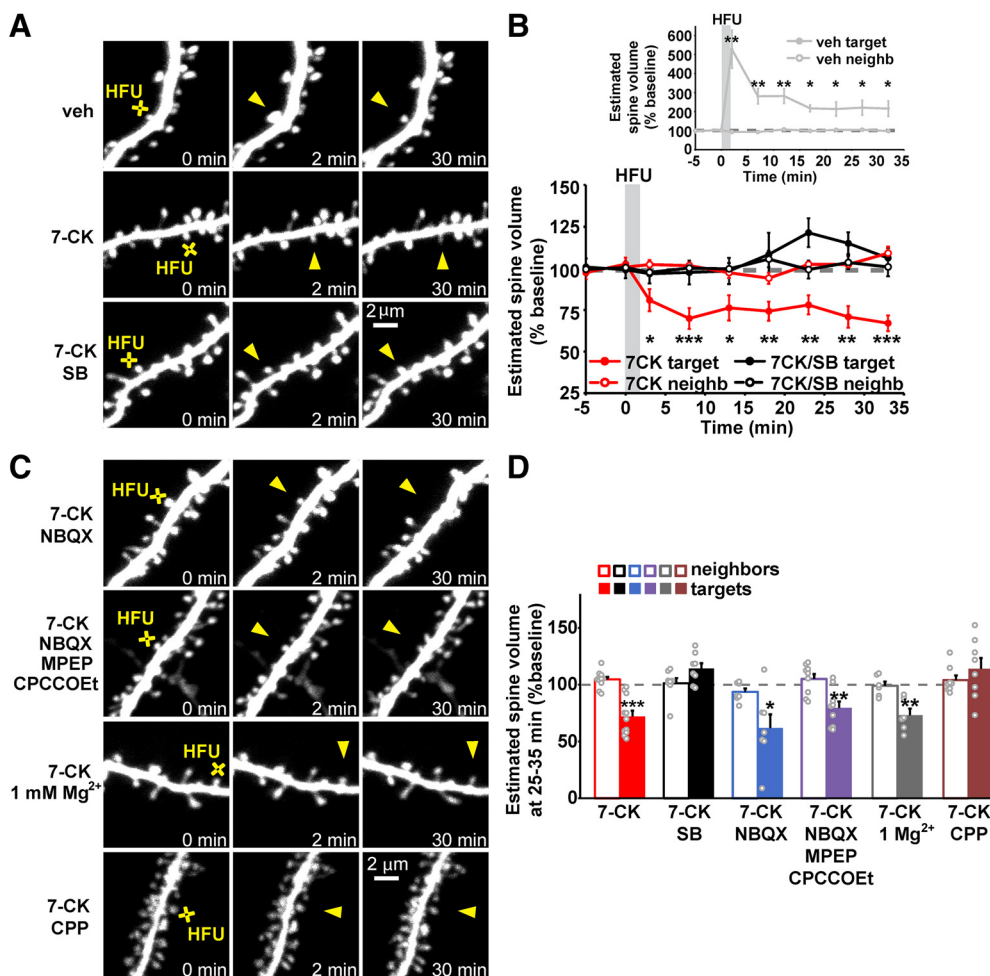


Figure 1. p38 MAPK activity is required for spine shrinkage driven by non-ionicotropic NMDAR signaling in response to high-frequency glutamate uncaging. **A**, Images of dendrites from EGFP-transfected CA1 neurons at 14–18 DIV before and after high-frequency glutamate uncaging (HFU, yellow cross) at individual dendritic spines (yellow arrowhead) in the presence of vehicle, 7-CK (100 μ M), and 7-CK with the p38 MAPK inhibitor SB203580 (SB; 2 μ M). **B**, HFU stimulation during vehicle conditions led to long-lasting spine growth (gray filled circles). In the presence of 7-CK, HFU induced dendritic spine shrinkage (red filled circles), which was blocked following inhibition of p38 MAPK activity with SB (black filled circles). The volume of unstimulated neighboring spines (open circles) was unaffected. **C**, Images of dendrites from EGFP-transfected CA1 neurons at 14–18 DIV before and after HFU (yellow cross) at individual dendritic spines (yellow arrowhead) in the presence of 7-CK with the AMPAR inhibitor NBQX (10 μ M), 7-CK with NBQX, and the group I mGluR inhibitors MPEP (15 μ M) and CPCCOEt (45 μ M), 7-CK in ACSF containing 1 mM Mg^{2+} , or 7-CK with CPP (10 μ M). **D**, Spine shrinkage was induced by HFU in the presence of 7-CK alone (red filled bar; 11 spines/11 cells) and 7-CK with NBQX (blue filled bar; 7 spines/7 cells), NBQX/MPEP/CPCCOEt (purple filled bar; 9 spines/9 cells), or 1 mM Mg^{2+} (gray filled bar; 6 spines/6 cells), but was blocked by SB203580 (black filled bar; 8 spines/8 cells) and by CPP (brown filled bar; 8 spines/8 cells). * $p < 0.05$, ** $p < 0.01$, *** $p < 0.001$, paired two-tailed t test compared with baseline and calculated across cells.

test), whereas the control peptide L-TAT-GASA, which does not compete with NOS1AP for the interaction with nNOS (Li et al., 2013), did not interfere with long-lasting dendritic spine shrinkage (Fig. 4A–C; $36.1 \pm 6.9\%$, $p < 0.0001$, $t_{(7)} = 9.26$). Importantly, neither the active peptide L-TAT-GESV nor the control peptide L-TAT-GASA affected the volume of unstimulated neighboring spines (Fig. 4A–C; 7-CK + L-TAT-GASA, $93.5 \pm 4.5\%$; 7-CK + L-TAT-GESV, $107.7 \pm 3.7\%$).

It is possible that nNOS simply functions as a scaffolding molecule to recruit NOS1AP into the NMDAR complex via its interactions with PSD-95 (Christopherson et al., 1999). Alternatively, nNOS enzymatic activity might be required for non-ionicotropic NMDAR signaling. We tested whether nNOS enzymatic activity is required using the NOS inhibitor L-NNA. We found that the application of L-NNA abolished HFU-induced non-ionicotropic NMDAR-dependent spine shrinkage (Fig. 4D–F; 7-CK: $69.2 \pm 7.6\%$, $p = 0.0002$, $t_{(12)} = 5.13$; 7-CK + L-NNA: $99.3 \pm 7.6\%$, $p = 0.38$, $t_{(10)} = 0.93$). Importantly, L-NNA did not affect the volume of unstimulated neighboring spines (Fig. 4D–F; 7-CK,

$105.7 \pm 5.1\%$; 7-CK + L-NNA, $103.9 \pm 5.7\%$). Together, our results support a model where non-ionicotropic NMDAR function drives dendritic spine shrinkage through nNOS activity and its interaction with NOS1AP.

MK2 activity and cofilin are required downstream of conformational NMDAR signaling to drive dendritic spine shrinkage

Spine shrinkage following LTD induction relies on remodeling of the spine actin cytoskeleton through the action of the actin depolymerizing protein cofilin (Zhou et al., 2004; Wang et al., 2007; Hayama et al., 2013). To shed light on how non-ionicotropic NMDAR signaling leads to remodeling of the actin cytoskeleton in spine shrinkage, we searched for signaling proteins that could link p38 MAPK to cofilin.

Interestingly, during mGluR-dependent LTD, a role for p38 MAPK and its downstream substrate MK2 was identified in the regulation of cofilin activity and dendritic spine morphology (Eales et al., 2014). We tested whether spine shrinkage driven by

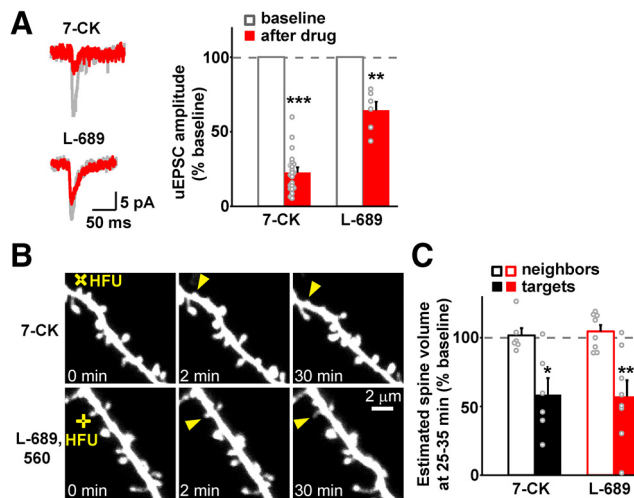


Figure 2. Spine shrinkage is induced by HFU in the presence of a lower concentration of L-689,560, which inhibits AMPARs to a lesser extent than 7-CK. **A**, Left, Representative uEPSCs from individual spines before (gray) and after (red) application of the NMDAR glycine/D-serine site antagonists 7-CK and L-689. Right, Application of 100 μ M 7-CK (22 spines/10 cells) greatly reduced and 10 μ M L-689 (6 spines/3 cells) partially reduced AMPAR uEPSCs (red filled bars). **B**, Representative images of dendrites from EGFP-transfected CA1 neurons at 14–18 DIV before and after HFU stimulation (yellow crosses) at individual dendritic spines (yellow arrowheads) in the presence of 100 μ M 7-CK or 10 μ M L-689. **C**, HFU stimulation in the presence of 7-CK (black bar; 6 spines/6 cells) or L-689 (red bar; 8 spines/8 cells) caused a stable decrease in spine size at 30 min. Volume of unstimulated neighboring spines (open bars) was not changed. * $p < 0.05$, ** $p < 0.01$, *** $p < 0.001$, paired two-tailed t test compared with baseline and calculated across spines in **A** and cells in **C**.

non-ionicotropic NMDAR signaling is dependent on MK2 activity. We found that spine shrinkage induced by HFU in the presence of 7-CK was blocked by application of MK2 inhibitor III (Fig. 5A–C; 7-CK: $70.5 \pm 6.4\%$, $p = 0.0012$, $t_{(9)} = 4.65$, paired two-tailed t test; 7-CK + MK2 inhibitor III: $105.5 \pm 11.7\%$, $p = 0.65$, $t_{(10)} = 0.47$). Importantly, MK2 inhibitor III did not affect the size of unstimulated neighboring spines (Fig. 5A–C; 7-CK, $93.9 \pm 3.9\%$; 7-CK + MK2 inhibitor III, $106.0 \pm 4.2\%$). Thus, MK2 activity is required for spine shrinkage driven by non-ionicotropic NMDAR signaling.

Furthermore, to confirm that cofilin is required downstream of this non-ionicotropic NMDAR-dependent and p38 MAPK-dependent signaling in spine shrinkage, we knocked down cofilin together with actin depolymerizing factor [ADF (a member of the cofilin protein family)] using previously published shRNA constructs (Bosch et al., 2014). We found that KD of cofilin and ADF blocked HFU-induced dendritic spine shrinkage in the presence of L-689 (Fig. 5D–F; shRNAs/L-689: $117.7 \pm 14.3\%$, $p = 0.25$, $t_{(8)} = 1.24$). Spine shrinkage was restored by coexpression of an shRNA-resistant version of wild-type cofilin (Fig. 5D–F; shRNAs + cofilin rescue/L-689: $67.8 \pm 4.1\%$, $p < 0.0001$, $t_{(10)} = 7.79$). Importantly, the size of unstimulated neighbors was not changed in either case (Fig. 5D–F; shRNAs/L-689, $108.6 \pm 5.6\%$; shRNAs + cofilin rescue/L-689, $105.1 \pm 6.1\%$). Thus, cofilin activation is required for spine shrinkage induced by non-ionicotropic NMDAR signaling.

We further investigated the role of cofilin by monitoring the redistribution of cofilin-GFP following induction of structural plasticity by HFU stimulation. Using cells coexpressing cofilin-GFP and the red cell fill CyRFP1, we simultaneously monitored changes in cofilin-GFP and spine volume. We found that there was no change in cofilin-GFP levels relative to spine volume immediately following HFU stimulation in the presence of 7-CK,

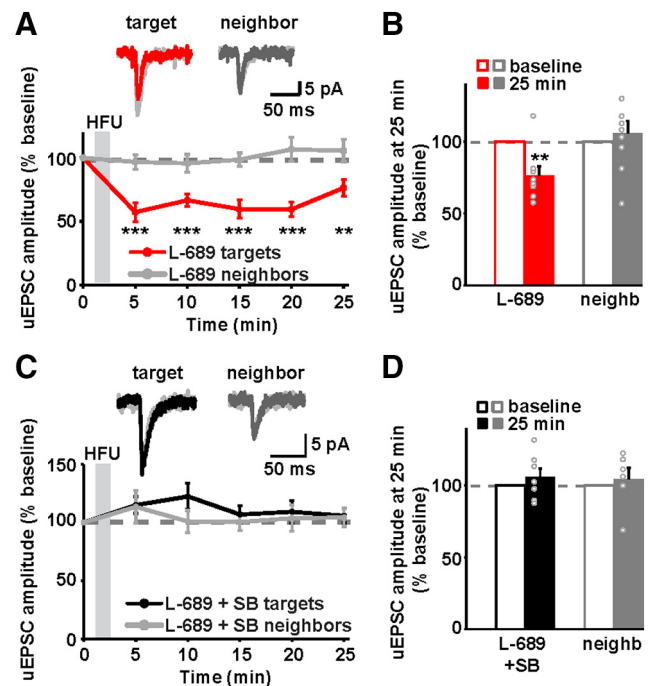


Figure 3. p38 MAPK activity is required for LTD driven by non-ionicotropic signaling through the NMDAR. **A**, Top, Representative uEPSCs from a target spine and an unstimulated neighbor before (light gray) and 25 min after HFU stimulation in the presence of L-689 (target, red; neighbor, dark gray). Bottom, Time course of averaged uEPSC amplitude compared with baseline. **B**, HFU stimulation in the presence of L-689 induced a long-lasting decrease in uEPSC amplitude of stimulated spines (red line/bar; 7 spines/7 cells), but not of unstimulated neighboring spines (gray line/bar). **C**, Top, Representative uEPSCs from a target spine and an unstimulated neighbor before (gray) and 25 min after HFU stimulation in the presence of L-689 and the p38 MAPK inhibitor SB (target, black; neighbor, dark gray). Bottom, Time course of averaged uEPSC amplitude compared with baseline. **D**, The p38 MAPK inhibitor SB blocked LTD induced by HFU in the presence of L-689 (black line/bar; 7 spines/7 cells), while the amplitude of uEPSCs from unstimulated neighboring spines (gray line/bar) did not change. ** $p < 0.01$, *** $p < 0.001$, paired two-tailed t test compared with baseline and calculated across cells.

but 10 min after uncaging the amount of cofilin-GFP decreased compared with spine volume and stayed decreased for at least up to 30 min (Fig. 6A,B; cofilin-GFP/CyRFP1 ratio at 25–35 min following HFU stimulation: $85.7 \pm 4.3\%$, $p < 0.0001$, $t_{(15)} = 6.44$, paired two-tailed t test). As a control, we show that during HFU-induced structural LTP, cofilin-GFP enriches in the stimulated spine for at least up to 30 min (Fig. 6C,D; cofilin-GFP/CyRFP1 ratio at 25–35 min following HFU stimulation: $217.1 \pm 43.3\%$, $p = 0.006$, $t_{(5)} = 4.65$), as reported previously (Bosch et al., 2014).

CaMKII activity is required for spine shrinkage driven by conformational NMDAR signaling

CaMKII has been shown to reposition within the NMDAR complex in response to non-ionicotropic NMDAR signaling (Aow et al., 2015), suggesting that it might play a role downstream of non-ionicotropic NMDAR signaling. Notably, CaMKII, which has been extensively studied in LTP induction (Bayer and Schulman, 2019), lately also has been implicated in LTD (Coultrap et al., 2014; Goodell et al., 2017; Woolfrey et al., 2018), further supporting a possible role in spine shrinkage downstream of non-ionicotropic NMDAR signaling.

We tested whether CaMKII is required for spine shrinkage driven by non-ionicotropic NMDAR signaling. We found that dendritic spine shrinkage induced by HFU in the presence of L-689 (Fig. 7A–C; L-689: $73.7 \pm 3.1\%$, $p < 0.0001$, $t_{(12)} = 8.37$,

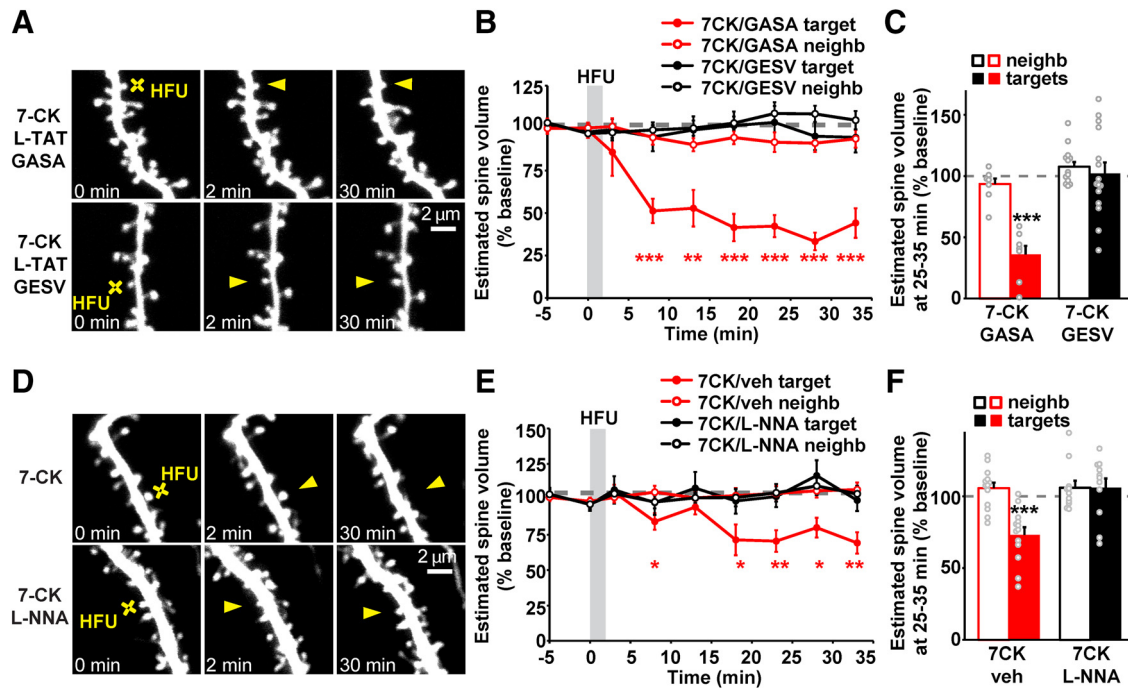


Figure 4. NOS1AP interaction with nNOS and nNOS enzymatic activity are required for spine shrinkage driven by non-ionotropic signaling through the NMDAR. **A**, Images of dendrites from EGFP-transfected CA1 neurons at 14–18 DIV before and after high-frequency glutamate uncaging (HFU, yellow cross) at an individual dendritic spine (yellow arrowhead) in the presence of 7-CK (100 μ M) and L-TAT-GASA (1 μ M) or L-TAT-GESV (1 μ M). **B**, **C**, Disruption of NOS1AP/nNOS interaction using the active cell-permeant L-TAT-GESV peptide (black filled circles/bar; 15 spines/15 cells), but not the inactive L-TAT-GASA control peptide (red filled circles/bar; 8 spines/8 cells), blocked spine shrinkage induced by non-ionotropic NMDAR signaling. Volume of unstimulated neighboring spines (open circles/bars) was unchanged. **D**, Images of dendrites from EGFP-transfected CA1 neurons at 14–18 DIV before and after HFU (yellow cross) at an individual dendritic spine (yellow arrowhead) in the presence of 7-CK (100 μ M) or 7-CK (100 μ M) and L-NNA (100 μ M). **E**, **F**, Inhibition of NO synthase activity with L-NNA blocked spine shrinkage (solid black circles/bar; 11 spines/11 cells) induced by HFU in the presence of 7-CK (solid red circles/bar; 13 spines/13 cells). The volume of unstimulated neighboring spines (open circles/bars) was unchanged. * $p < 0.05$, ** $p < 0.01$, *** $p < 0.001$, paired two-tailed t test compared with baseline and calculated across cells.

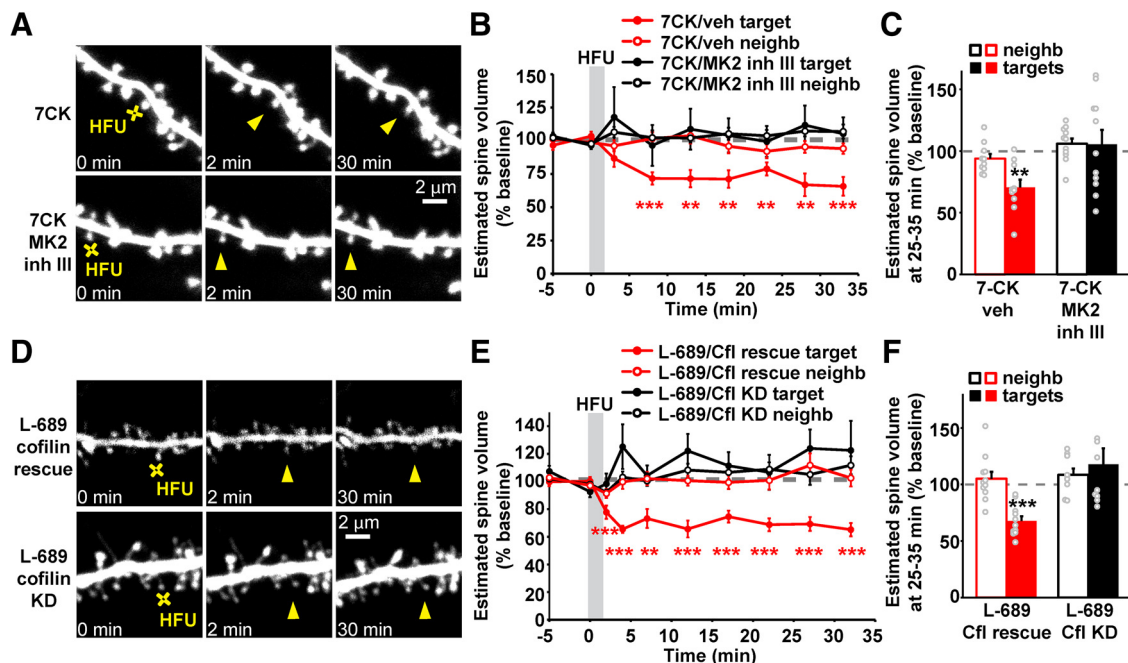


Figure 5. MK2 activity and cofilin are required for spine shrinkage driven by non-ionotropic NMDAR signaling. **A**, Images of dendrites from EGFP-expressing neurons (14–18 DIV) showing spine shrinkage (yellow arrowheads) induced by HFU (yellow crosses) in the presence of 7-CK and MK2 inhibitor III (10 μ M). **B**, **C**, Inhibition of MK2 activity (black filled circles/bar; 11 spines/11 cells) prevented spine shrinkage induced by HFU in the presence of 7-CK (red filled circles/bar; 10 spines/10 cells). Volume of unstimulated neighboring spines (open circles/bars) did not change. **D**, Images of dendrites from 14–18 DIV neurons expressing CyRFP1 with EGFP and cofilin and ADF shRNAs (KD) or cofilin and ADF shRNAs together with shRNA-resistant cofilin-EGFP (rescue) before and after HFU (yellow crosses) at a single dendritic spine (yellow arrowheads) in the presence of L-689 (10 μ M). **E**, **F**, KD of cofilin and ADF (black filled circles/bar; 11 spines/11 cells) blocked non-ionotropic NMDAR-dependent spine shrinkage in the presence of L-689 and was rescued by shRNA-resistant cofilin-EGFP (red filled circles/bar; 9 spines/9 cells). Volume of unstimulated neighboring spines (open circles/bars) was not changed. ** $p < 0.01$, *** $p < 0.001$, paired two-tailed t test compared with baseline and calculated across cells.

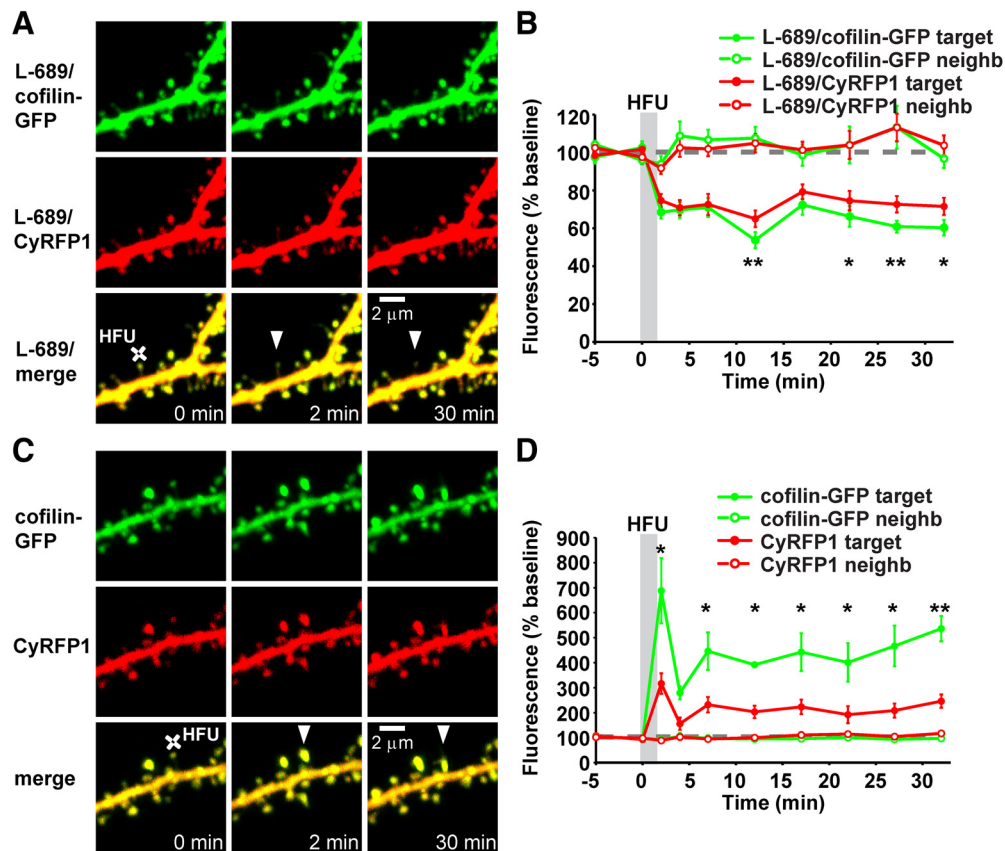


Figure 6. Non-ionotropic NMDAR-dependent spine shrinkage is associated with loss of cofilin from the spine head. **A**, Images of CA1 neurons transfected with cofilin shRNAs in combination with shRNA-resistant cofilin-EGFP and CyRFP1 before and after HFU (white crosses) at individual spines (white arrowheads) in the presence of L-689. **B**, Spine shrinkage (red, CyRFP1) induced by HFU in the presence of L-689 was associated with a decrease of cofilin-GFP protein levels in the spine (green). Cofilin-GFP spine levels were decreased 10 min after HFU in L-689 and stayed decreased until 30 min after HFU in L-689 (16 spines/16 cells). **C**, Images of dendrites from 14–18 DIV CA1 neurons expressing cofilin shRNAs in combination with shRNA-resistant cofilin-EGFP and CyRFP1 before and after HFU (white crosses) at individual spines (white arrowheads). **D**, Time course of HFU-induced changes in spine volume (red, CyRFP1) and the amount of cofilin-GFP protein in the spine (green) compared with baseline. Cofilin-GFP spine levels were enriched after HFU and remained enriched for at least 30 min following HFU (6 spines/6 cells). * $p < 0.05$, ** $p < 0.01$, paired two-tailed t test, comparison of cofilin-EGFP to CyRFP1, calculated across cells.

paired two-tailed t test) was blocked in the presence of KN-62 (Fig. 7A–C; L-689 + KN-62: $92.9 \pm 4.4\%$, $p = 0.15$, $t_{(8)} = 1.61$) or TAT-CN21 (Fig. 7A–C; L-689 + TAT-CN21: $102.8 \pm 5.2\%$, $p = 0.60$, $t_{(8)} = 0.54$). Importantly, the size of unstimulated neighboring spines was not affected (Fig. 7A–C; L-689, $95.3 \pm 5.0\%$; L-689 + KN-62, $90.3 \pm 2.4\%$; L-689 + TAT-CN21, $102.1 \pm 4.3\%$). Our results demonstrate that CaMKII is required for dendritic spine shrinkage induced by non-ionotropic NMDAR signaling.

Discussion

Molecular mechanisms of non-ionotropic NMDAR signaling

Despite several recent studies demonstrating that the NMDAR can signal independent of ion flow to drive dendritic spine shrinkage and LTD (Nabavi et al., 2013; Aow et al., 2015; Stein et al., 2015; Carter and Jahr, 2016; Wong and Gray, 2018), the molecular signaling mechanisms that link conformational NMDAR signaling to LTD and spine shrinkage remained poorly defined. Here, we have identified several components of key importance in this signaling cascade (Fig. 7D).

p38 MAPK

Only one protein, p38 MAPK, had previously been implicated as a downstream component of non-ionotropic NMDAR signaling; first, shown to be phosphorylated downstream of non-ionotropic NMDAR function in chemically induced LTD (Nabavi et al.,

2013); and second, shown to be required for spine shrinkage driven by non-ionotropic NMDAR signaling induced by low-frequency glutamatergic stimulation (Stein et al., 2015). Here, we identify p38 MAPK as generally being required for non-ionotropic NMDAR signaling during synaptic plasticity. We show that p38 MAPK is required for both (1) spine shrinkage and (2) long-term depression of synaptic currents induced by high-frequency glutamatergic stimulation in the presence of the glycine/D-serine site NMDAR antagonists 7-CK and L-689. Combined, these results confirm a key role for p38 MAPK in the signaling cascade driven by conformational signaling by the NMDAR. As p38 MAPK has been implicated in classical LFS-induced LTD (Zhu et al., 2002), the molecular signaling mechanisms studied here likely also contribute to classical NMDAR-mediated LTD.

NOS1AP and nNOS

We identified a novel role for the interaction between NOS1AP and nNOS, likely upstream of p38 MAPK, in spine shrinkage induced by non-ionotropic NMDAR signaling. We propose that the recruitment of NOS1AP to nNOS could be important for localized activation of p38 MAPK, and thus for phosphorylation of proteins driving spine shrinkage and AMPAR endocytosis. Indeed, it has been shown that NOS1AP interacts with the p38 MAPK activator MKK3 and that, during NMDA-induced excitotoxicity, NOS1AP interactions with nNOS and MKK3 are required for p38 MAPK activation (Li et al., 2013). As p38

MAPK is linked to PSD-95 and the NMDAR complex, p38 MAPK could participate with Rap1 in microdomain-specific signaling at late endosomes and thus could phosphorylate GluA2, disrupting AMPAR anchoring (Chung et al., 2000; Zhang et al., 2018a) and leading to LTD and spine shrinkage.

Notably, NOS1AP is important for nNOS-mediated nitrosylation of Dexas1, a small GTPase that negatively regulates the MAP kinase Erk (Zhu et al., 2014; Zhang et al., 2018b). Thus, the dual and opposite regulation of p38 and Erk MAPK activities through NOS1AP would allow NOS1AP to locally activate p38 MAPK-dependent LTD and spine shrinkage signaling pathways, and at the same time downregulate Erk-dependent LTP signaling (Zhu et al., 2002; Zhang et al., 2018a). Alternatively, the effects of Dexas1 on Erk activity could be independent of the fast activity-induced recruitment of NOS1AP and up-regulation of p38 MAPK activity, as changes in Erk activity were reported only after long-term treatments.

nNOS is considered a calcium-dependent enzyme, yet we found that nNOS is required downstream of non-ionotropic NMDAR signaling, which is not associated with ion flux or detectable calcium transients (Stein et al., 2015). Notably, Nabavi et al. (2013) showed that non-ionotropic NMDAR signaling was sufficient to induce LTD even when intracellular calcium was clamped at basal levels with calcium chelators. Thus, we propose that basal calcium is sufficient to support nNOS activity. However, conformational NMDAR signaling could also activate nNOS via an undetectable calcium source.

MK2 and cofilin

Downstream of glutamate-induced conformational changes in the NMDAR (Dore et al., 2015; Ferreira et al., 2017), we showed that the p38 MAPK substrate MK2 and cofilin are required for non-ionotropic NMDAR-dependent spine shrinkage. The signaling pathways downstream of p38 MAPK leading to spine shrinkage and LTD are expected to ultimately diverge, as cofilin previously has been implicated in spine shrinkage and elimination, but not LTD (Zhou et al., 2004; Wang et al., 2007).

Earlier studies showed that MK2 is activated by p38 MAPK during DHPG [(S)-3,5-dihydroxyphenylglycine]-induced mGluR-dependent LTD, leading to dephosphorylation and activation of cofilin in a p38 MAPK-dependent manner (Eales et al., 2014). We propose that during conformational NMDAR signaling activated p38 MAPK also binds and phosphorylates MK2, which then activates cofilin. Yet how the activation of MK2 is linked to decreased cofilin phosphorylation remains unclear. The severing and depolymerization activity of cofilin is regulated by the phosphorylation on Ser3 through an interplay of the deactivating kinase LIMK1 and the phosphatase slingshot (Ohashi, 2015). In endothelial cells

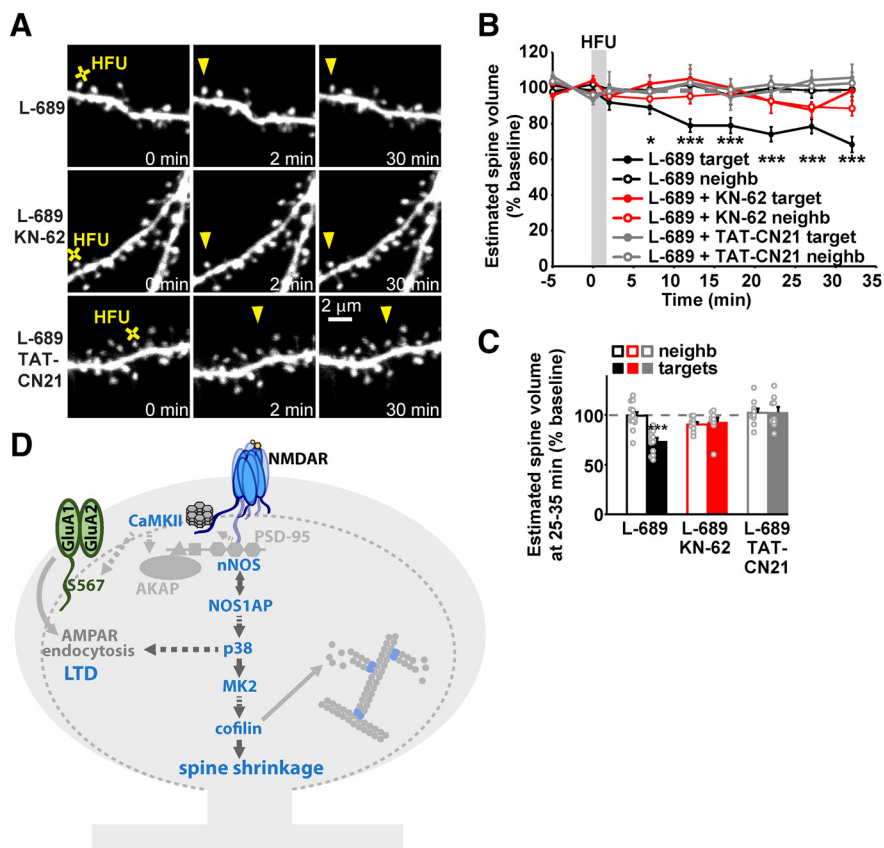


Figure 7. CaMKII activity is required for spine shrinkage driven by non-ionotropic NMDAR signaling. **A**, Images of dendrites from CA1 neurons of acute slices from P16 to P20 GFP-M mice before and after HFU (yellow cross) at single spines (yellow arrowhead) in the presence of L-689, L-689 with 10 μ M KN-62, or L-689 with 5 μ M TAT-CN21. **B**, **C**, Inhibition of CaMKII activity with KN-62 (red filled circles/bar; 9 spines/9 cells) or TAT-CN21 (gray filled circles/bar; 9 spines/9 cells) blocked spine shrinkage induced by HFU in the presence of L-689 (black filled circles/bar; 8 spines/8 cells). Volume of unstimulated neighboring spines (open bars) was not changed. * $p < 0.05$, ** $p < 0.001$, paired two-tailed t test compared with baseline and calculated across cells. **D**, Proposed model for the non-ionotropic NMDAR signaling pathway that drives spine shrinkage. Glutamate binding to the NMDAR induces conformational changes that drive dendritic spine shrinkage through NOS1AP–nNOS interactions, and the activities of nNOS, p38 MAPK, MK2, CaMKII, and cofilin-dependent severing of the actin cytoskeleton.

MK2 has been shown to phosphorylate and activate LIMK1 (Kobayashi et al., 2006; Scott and Olson, 2007). Thus, increases in LIMK1 phosphorylation caused by MK2 activation and the subsequent F-actin stabilization could activate slingshot, which could dephosphorylate LIMK1 and cofilin, driving spine shrinkage and retraction.

Alternatively, MK2 could act on a target independent of LIMK1, as observed during bone morphogenetic protein-2-induced cell migration (Gamell et al., 2011). In contrast to LIMK1, not much is known about synapse-specific pathways regulating slingshot activity, drawing attention to other phosphatases like PP1, which have also been shown to activate cofilin (Ohashi, 2015; Shaw and Bamberg, 2017). In addition, the phosphatase PP2B, which at basal activity levels is required for non-ionotropic NMDAR signaling (Nabavi et al., 2013), can partner with slingshot for F-actin reorganization during spine retraction (Zhou et al., 2012).

CaMKII

Here we show that CaMKII activity is required for spine shrinkage driven by non-ionotropic NMDAR signaling. This may appear surprising as the majority of studies on CaMKII have focused on its role in LTP and spine growth (Bayer and

Schulman, 2019) and, like nNOS, CaMKII is considered a calcium-dependent enzyme. Notably, several recent studies have revealed a role of CaMKII in LTD (Coultrap et al., 2014; Goodell et al., 2017; Woolfrey et al., 2018). We propose that basal calcium is sufficient to support enzymatic activity during non-ionotropic NMDAR signaling. Indeed, LTD requires autonomous CaMKII activity (Coultrap et al., 2014), which enables the kinase to stay active past a previous calcium signal. Therefore, autonomous CaMKII activity required for dendritic spine shrinkage could be mediated by a NMDAR-bound autonomous active CaMKII pool, independent of concurrent calcium influx. Moreover, CaMKII autonomous activity could be induced through nitrosylation of Cys-280/289 (Coultrap and Bayer, 2014); however, we think this is unlikely, as during LTD an increase in T286 phosphorylation was reported (Coultrap et al., 2014), whereas T286 phosphorylation is reduced following nitrosylation (Coultrap and Bayer, 2014).

What role does CaMKII play in non-ionotropic NMDAR signaling? We propose that the NMDAR conformational change could move NMDAR-bound CaMKII closer to alternative substrates. Indeed, in the LTD studies, autonomously active CaMKII was shown to have different substrate selectivity than when Ca^{2+} /CaM is bound, targeting nontraditional substrates like AKAP79/150 or GluA1 S567 to mediate LTD (Coultrap et al., 2014; Woolfrey et al., 2018). However, in contrast with these studies, it has been observed that CaMKII bound to the NMDAR exhibits decreased autonomous activity, accompanied by a delayed repositioning within the receptor complex (Aow et al., 2015). Perhaps CaMKII repositioning within the NMDAR complex and T286 dephosphorylation acts as a safeguard to limit autonomous CaMKII activity during non-ionotropic NMDAR signaling.

Alternatively, or additionally, CaMKII may have a structural role in the non-ionotropic NMDAR signaling pathway through its interaction with F-actin. Release of the stabilizing CaMKII–actin interaction is crucial for both LTP and spine growth by allowing actin-regulating proteins like cofilin to bind to F-actin (Hell, 2014; Kim et al., 2015). Because non-ionotropic NMDAR signaling requires cofilin activity to drive spine shrinkage, we expect that CaMKII–actin interaction must be released as well.

Non-ionotropic NMDAR signaling in disease

We identified a novel role for the interaction of NOS1AP and nNOS in spine shrinkage driven by non-ionotropic NMDAR signaling. Notably, both nNOS and NOS1AP have been identified as schizophrenia risk genes (Shinkai et al., 2002; Freudenberg et al., 2015). Our findings raise the question of whether NOS1AP-mediated signaling contributes to the spine loss associated with schizophrenia. Intriguingly, reduced levels of the synaptic NMDAR coagonist D-serine and polymorphisms of genes involved in the regulation of D-serine levels have been found in patients with schizophrenia (Hashimoto et al., 2005; Goltsov et al., 2006; Balu et al., 2013). These pathologic conditions could result in a shift toward increased non-ionotropic NMDAR signaling and could contribute to the decreased spine density observed in patients with schizophrenia (Penzes et al., 2011; Glausier and Lewis, 2013).

Several earlier studies have implicated non-ionotropic NMDAR signaling in Alzheimer's disease (Kessels et al., 2013; Tamburri et al., 2013; Birnbaum et al., 2015), which is associated with dendritic spine loss (Selkoe, 2002). Notably, p38 MAPK activity was linked to amyloid β ($A\beta$)-induced spine loss driven by non-ionotropic NMDAR signaling (Birnbaum et al., 2015). In addition, increased nNOS–NOS1AP interaction was detected

after treatment with $A\beta$ *in vitro* and in APP/PS1 mice *in vivo* (Zhang et al., 2018b). After blocking the nNOS–NOS1AP interaction, memory was rescued in 4-month-old APP/PS1 mice, and dendritic impairments were ameliorated both *in vivo* and *in vitro* (Zhang et al., 2018b), further supporting a role for non-ionotropic NMDAR signaling in Alzheimer's disease.

References

- Aow J, Dore K, Malinow R (2015) Conformational signaling required for synaptic plasticity by the NMDA receptor complex. *Proc Natl Acad Sci U S A* 112:14711–14716.
- Babiec WE, Guglietta R, Jami SA, Morishita W, Malenka RC, O'Dell TJ (2014) Ionotropic NMDA receptor signaling is required for the induction of long-term depression in the mouse hippocampal CA1 region. *J Neurosci* 34:5285–5290.
- Balu DT, Li Y, Puhl MD, Benneyworth MA, Basu AC, Takagi S, Bolshakov VY, Coyle JT (2013) Multiple risk pathways for schizophrenia converge in serine racemase knockout mice, a mouse model of NMDA receptor hypofunction. *Proc Natl Acad Sci U S A* 110:E2400–E2409.
- Bayer KU, Schulman H (2019) CaM Kinase: still inspiring at 40. *Neuron* 103:380–394.
- Birnbaum JH, Bali J, Rajendran L, Nitsch RM, Tackenberg C (2015) Calcium flux-independent NMDA receptor activity is required for Abeta oligomer-induced synaptic loss. *Cell Death Dis* 6:e1791.
- Bosch M, Castro J, Saneyoshi T, Matsuno H, Sur M, Hayashi Y (2014) Structural and molecular remodeling of dendritic spine substructures during long-term potentiation. *Neuron* 82:444–459.
- Carter BC, Jahr CE (2016) Postsynaptic, not presynaptic NMDA receptors are required for spike-timing-dependent LTD induction. *Nat Neurosci* 19:1218–1224.
- Christopherson KS, Hillier BJ, Lim WA, Brecht DS (1999) PSD-95 assembles a ternary complex with the N-methyl-D-aspartic acid receptor and a bivalent neuronal NO synthase PDZ domain. *J Biol Chem* 274:27467–27473.
- Chung HJ, Xia J, Scannevin RH, Zhang X, Hagan RL (2000) Phosphorylation of the AMPA receptor subunit GluR2 differentially regulates its interaction with PDZ domain-containing proteins. *J Neurosci* 20:7258–7267.
- Coultrap SJ, Bayer KU (2014) Nitric oxide induces Ca^{2+} -independent activity of the Ca^{2+} /calmodulin-dependent protein kinase II (CaMKII). *J Biol Chem* 289:19458–19465.
- Coultrap SJ, Freund RK, O'Leary H, Sanderson JL, Roche KW, Dell'Acqua ML, Bayer KU (2014) Autonomous CaMKII mediates both LTP and LTD using a mechanism for differential substrate site selection. *Cell Rep* 6:431–437.
- Dore K, Aow J, Malinow R (2015) Agonist binding to the NMDA receptor drives movement of its cytoplasmic domain without ion flow. *Proc Natl Acad Sci U S A* 112:14705–14710.
- Eales KL, Palygin O, O'Loughlin T, Rasooli-Nejad S, Gaestel M, Müller J, Collins DR, Pankratov Y, Corrèa SAL (2014) The MK2/3 cascade regulates AMPAR trafficking and cognitive flexibility. *Nat Commun* 5:4701.
- Feng G, Mellor RH, Bernstein M, Keller-Peck C, Nguyen QT, Wallace M, Nerbonne JM, Lichtman JW, Sanes JR (2000) Imaging neuronal subsets in transgenic mice expressing multiple spectral variants of GFP. *Neuron* 28:41–51.
- Ferreira JS, Papouin T, Ladépêche L, Yao A, Langlais VC, Bouchet D, Dulong J, Mothet JP, Sacchi S, Pollegioni L, Paoletti P, Oliet SHR, Groc L (2017) Co-agonists differentially tune GluN2B-NMDA receptor trafficking at hippocampal synapses. *Elife* 6:e25492.
- Freudenberg F, Althoff A, Reif A (2015) Neuronal nitric oxide synthase (NOS1) and its adaptor, NOS1AP, as a genetic risk factors for psychiatric disorders. *Genes Brain Behav* 14:46–63.
- Gamell C, Susperregui AG, Bernard O, Rosa JL, Ventura F (2011) The p38/MK2/Hsp25 pathway is required for BMP-2-induced cell migration. *PLoS One* 6:e16477.
- Glausier JR, Lewis DA (2013) Dendritic spine pathology in schizophrenia. *Neuroscience* 251:90–107.
- Goltsov AY, Loseva JG, Andreeva TV, Grigorenko AP, Abramova LI, Kaleda VG, Orlova VA, Moliaka YK, Rogav EI (2006) Polymorphism in the 5'-promoter region of serine racemase gene in schizophrenia. *Mol Psychiatry* 11:325–326.

- Goodell DJ, Zaegel V, Coultrap SJ, Hell JW, Bayer KU (2017) DAPK1 mediates LTD by making CaMKII/GluN2B binding LTP specific. *Cell Rep* 19:2231–2243.
- Hashimoto K, Engberg G, Shimizu E, Nordin C, Lindström LH, Iyo M (2005) Reduced D-serine to total serine ratio in the cerebrospinal fluid of drug naive schizophrenic patients. *Prog Neuropsychopharmacol Biol Psychiatry* 29:767–769.
- Hayama T, Noguchi J, Watanabe S, Takahashi N, Hayashi-Takagi A, Ellis-Davies GC, Matsuzaki M, Kasai H (2013) GABA promotes the competitive selection of dendritic spines by controlling local Ca²⁺ signaling. *Nat Neurosci* 16:1409–1416.
- Hell JW (2014) CaMKII: claiming center stage in postsynaptic function and organization. *Neuron* 81:249–265.
- Holtmaat AJ, Trachtenberg JT, Wilbrecht L, Shepherd GM, Zhang X, Knott GW, Svoboda K (2005) Transient and persistent dendritic spines in the neocortex in vivo. *Neuron* 45:279–291.
- Kessels HW, Nabavi S, Malinow R (2013) Metabotropic NMDA receptor function is required for β -amyloid-induced synaptic depression. *Proc Natl Acad Sci U S A* 110:4033–4038.
- Kim K, Lakhanpal G, Lu HE, Khan M, Suzuki A, Hayashi MK, Narayanan R, Luyben TT, Matsuda T, Nagai T, Blanpied TA, Hayashi Y, Okamoto K (2015) A temporary gating of actin remodeling during synaptic plasticity consists of the interplay between the kinase and structural functions of CaMKII. *Neuron* 87:813–826.
- Kobayashi M, Nishita M, Mishima T, Ohashi K, Mizuno K (2006) MAPKAPK-2-mediated LIM-kinase activation is critical for VEGF-induced actin remodeling and cell migration. *EMBO J* 25:713–726.
- Lai CS, Franke TF, Gan WB (2012) Opposite effects of fear conditioning and extinction on dendritic spine remodeling. *Nature* 483:87–91.
- Laviv T, Kim BB, Chu J, Lam AJ, Lin MZ, Yasuda R (2016) Simultaneous dual-color fluorescence lifetime imaging with novel red-shifted fluorescent proteins. *Nat Methods* 13:989–992.
- Leeson PD, Carling RW, Moore KW, Moseley AM, Smith JD, Stevenson G, Chan T, Baker R, Foster AC, Grimwood S (1992) 4-Amido-2-carboxy-tetrahydroquinolines. Structure-activity relationships for antagonism at the glycine site of the NMDA receptor. *J Med Chem* 35:1954–1968.
- Li LL, Ginot V, Liu X, Vergun O, Tuittila M, Mathieu M, Bonny C, Puyal J, Truttmann AC, Courtney MJ (2013) The nNOS-p38MAPK pathway is mediated by NOS1AP during neuronal death. *J Neurosci* 33:8185–8201.
- Li LL, Melero-Fernandez de Mera RM, Chen J, Ba W, Kasri NN, Zhang M, Courtney MJ (2015) Unexpected heterodivalent recruitment of NOS1AP to nNOS reveals multiple sites for pharmacological intervention in neuronal disease models. *J Neurosci* 35:7349–7364.
- Nabavi S, Kessels HW, Alfonso S, Aow J, Fox R, Malinow R (2013) Metabotropic NMDA receptor function is required for NMDA receptor-dependent long-term depression. *Proc Natl Acad Sci U S A* 110:4027–4032.
- Oh WC, Hill TC, Zito K (2013) Synapse-specific and size-dependent mechanisms of spine structural plasticity accompanying synaptic weakening. *Proc Natl Acad Sci U S A* 110:E305–E312.
- Ohashi K (2015) Roles of cofilin in development and its mechanisms of regulation. *Dev Growth Differ* 57:275–290.
- Okamoto K, Nagai T, Miyawaki A, Hayashi Y (2004) Rapid and persistent modulation of actin dynamics regulates postsynaptic reorganization underlying bidirectional plasticity. *Nat Neurosci* 7:1104–1112.
- Penzes P, Cahill ME, Jones KA, VanLeeuwen JE, Woolfrey KM (2011) Dendritic spine pathology in neuropsychiatric disorders. *Nat Neurosci* 14:285–293.
- Pologruto TA, Sabatini BL, Svoboda K (2003) ScanImage: flexible software for operating laser scanning microscopes. *Biomed Eng Online* 2:13.
- Ramiro-Cortés Y, Israely I (2013) Long lasting protein synthesis- and activity-dependent spine shrinkage and elimination after synaptic depression. *PLoS One* 8:e71155.
- Sanderson JL, Gorski JA, Dell'Acqua ML (2016) NMDA receptor-dependent LTD requires transient synaptic incorporation of Ca²⁺-permeable AMPARs mediated by AKAP150-anchored PKA and calcineurin. *Neuron* 89:1000–1015.
- Scott RW, Olson MF (2007) LIM kinases: function, regulation and association with human disease. *J Mol Med (Berl)* 85:555–568.
- Selkoe DJ (2002) Alzheimer's disease is a synaptic failure. *Science* 298:789–791.
- Shaw AE, Bamberg JR (2017) Peptide regulation of cofilin activity in the CNS: a novel therapeutic approach for treatment of multiple neurological disorders. *Pharmacol Ther* 175:17–27.
- Shinkai T, Ohmori O, Hori H, Nakamura J (2002) Allelic association of the neuronal nitric oxide synthase (NOS1) gene with schizophrenia. *Mol Psychiatry* 7:560–563.
- Stein IS, Gray JA, Zito K (2015) Non-ionotropic nmda receptor signaling drives activity-induced dendritic spine shrinkage. *J Neurosci* 35:12303–12308.
- Stoppini L, Buchs PA, Muller D (1991) A simple method for organotypic cultures of nervous tissue. *J Neurosci Methods* 37:173–182.
- Tamburri A, Dudilot A, Licea S, Bourgeois C, Boehm J (2013) NMDA-receptor activation but not ion flux is required for amyloid-beta induced synaptic depression. *PLoS One* 8:e65350.
- Volianskis A, France G, Jensen MS, Bortolotto ZA, Jane DE, Collingridge GL (2015) Long-term potentiation and the role of N-methyl-D-aspartate receptors. *Brain Res* 1621:5–16.
- Wang XB, Yang Y, Zhou Q (2007) Independent expression of synaptic and morphological plasticity associated with long-term depression. *J Neurosci* 27:12419–12429.
- Wiegert JS, Oertner TG (2013) Long-term depression triggers the selective elimination of weakly integrated synapses. *Proc Natl Acad Sci U S A* 110:E4510–E4519.
- Wilkerson JR, Albanesi JP, Huber KM (2018) Roles for Arc in metabotropic glutamate receptor-dependent LTD and synapse elimination: implications in health and disease. *Semin Cell Dev Biol* 77:51–62.
- Wise SP, Fleshman JW Jr, Jones EG (1979) Maturation of pyramidal cell form in relation to developing afferent and efferent connections of rat somatic sensory cortex. *Neuroscience* 4:1275–1297.
- Wong JM, Gray JA (2018) Long-term depression is independent of GluN2 subunit composition. *J Neurosci* 38:4462–4470.
- Woods G, Zito K (2008) Preparation of gene gun bullets and biolistic transfection of neurons in slice culture. *J Vis Exp. Advance online publication*. Retrieved February 13, 2008. doi: 10.3791/675.
- Woods GF, Oh WC, Boudewyn LC, Mikula SK, Zito K (2011) Loss of PSD-95 enrichment is not a prerequisite for spine retraction. *J Neurosci* 31:12129–12138.
- Woolfrey KM, O'Leary H, Goodell DJ, Robertson HR, Horne EA, Coultrap SJ, Dell'Acqua ML, Bayer KU (2018) CaMKII regulates the dephosphorylation and synaptic removal of the scaffold protein AKAP79/150 to mediate structural long-term depression. *J Biol Chem* 293:1551–1567.
- Yang G, Pan F, Gan WB (2009) Stably maintained dendritic spines are associated with lifelong memories. *Nature* 462:920–924.
- Zhang L, Zhang P, Wang G, Zhang H, Zhang Y, Yu Y, Zhang M, Xiao J, Crespo P, Hell JW, Lin L, Hugarin RL, Zhu JJ (2018a) Ras and Rap signal bidirectional synaptic plasticity via distinct subcellular microdomains. *Neuron* 98:783–800.e4.
- Zhang Y, Zhu Z, Liang HY, Zhang L, Zhou QG, Ni HY, Luo CX, Zhu DY (2018b) nNOS-CAPON interaction mediates amyloid- β -induced neurotoxicity, especially in the early stages. *Aging Cell* 17:e12754.
- Zhou L, Jones EV, Murai KK (2012) EphA signaling promotes actin-based dendritic spine remodeling through slingshot phosphatase. *J Biol Chem* 287:9346–9359.
- Zhou Q, Homma KJ, Poo MM (2004) Shrinkage of dendritic spines associated with long-term depression of hippocampal synapses. *Neuron* 44:749–757.
- Zhu JJ, Qin Y, Zhao M, Van Aelst L, Malinow R (2002) Ras and Rap control AMPA receptor trafficking during synaptic plasticity. *Cell* 110:443–455.
- Zhu LJ, Li TY, Luo CX, Jiang N, Chang L, Lin YH, Zhou HH, Chen C, Zhang Y, Lu W, Gao LY, Ma Y, Zhou QG, Hu Q, Hu XL, Zhang J, Wu HY, Zhu DY (2014) CAPON-nNOS coupling can serve as a target for developing new anxiolytics. *Nat Med* 20:1050–1054.
- Zuo Y, Lin A, Chang P, Gan WB (2005) Development of long-term dendritic spine stability in diverse regions of cerebral cortex. *Neuron* 46:181–189.